Hindawi
Journal of Mathematics
Volume 2022, Article ID 8043131, 13 pages
https://doi.org/10.1155/2022/8043131

Research Article

Dynamic Analysis of an HIV Model Incorporating Cytotoxic T Lymphocytes and Vectored Immunoprophylaxis

Hongyan Chen[1] **and Jianfeng Luo**[2]

[1]*Chongqing Vocational Institute of Engineering, Chongqing 402260, China*
[2]*The Hong Kong Polytechnic University Shenzhen Research Institute, Shenzhen 518000, China*

Correspondence should be addressed to Jianfeng Luo; gstljf@polyu.edu.hk

Received 14 April 2022; Revised 15 August 2022; Accepted 15 September 2022; Published 27 September 2022

Academic Editor: G Muhiuddin

The objective of this study is to investigate the effects of immune responses on HIV replication by using a novel HIV model that incorporates immune responses including cytotoxic T lymphocytes and antibodies. In this model, the cytotoxic lymphocyte cells are stimulated by infected T cells, and the antibodies are received continuously through vectored immunoprophylaxis. In the first step, we analyze the well-posedness of our proposed model. By obtaining the basic reproduction number, we also investigate the existence of equilibrium in three cases, including infection-free equilibrium, immune-free infection equilibrium, and immune-present infection equilibrium. As a result, we demonstrate our model can admit two immune-free infection equilibria, which are dependent on the basic reproduction number. Additionally, we study their local stability and find sufficient conditions for them. In particular, we show that immune-free infection equilibrium and immune-present infection equilibrium can become unstable from stable, and then a simple Hopf bifurcation can occur. Theoretical results about backward bifurcation and forward bifurcation are further derived. In addition, simulations reveal rich dynamic behaviors, such as backward bifurcation, forward bifurcation, and Hopf bifurcation. The rich dynamics of the proposed model demonstrate the importance and complexity of immune responses when fighting HIV replication.

1. Introduction and Model

As the human immunodeficiency virus (HIV) emerged in the early 1980s, it quickly became a worldwide health issue, due to its infectiousness, mortality, and incurability. Biological studies have shown that HIV infects $CD4^+$ T helper cells and attacks the immune system, causing the body to lose immunity. Humans are therefore susceptible to a variety of diseases, as well as malignant tumors. Therefore, revealing the HIV replication mechanism in vivo and predicting the impacts of interventions can help humans improve survival and reduce the therapy cost. Considering these two scenarios, mathematical models are imperative to reduce the cost and control virus replication. For example, the authors in [1–3] study COVID-19 and estimate the impacts of intervention strategies by mathematical models, which provides significant theoretical guidance for the process of human antiviral.

It is clear that many scholars also studied HIV replication mechanism by mathematical models. Nowak and Bangham [4, 5] proposed a basic model to describe the variation of the virus in vivo:

$$\begin{aligned}\frac{dT}{dt} &= \Lambda - \delta_1 T - \beta_1 VT,\\ \frac{dT^*}{dt} &= \beta VT - \delta_2 T^*,\\ \frac{dV}{dt} &= N\delta_2 T^* - \delta_3 V,\end{aligned} \tag{1}$$

where T denotes the concentration of helper T cells, T^* denotes the concentration of infected helper T cells, and V denotes the concentration of the virus. Λ is the production rate of new target cells. δ_1 and δ_2 are the death rates of

uninfected cells and infected cells, respectively. β_1 is the infection coefficient, and N is the burst coefficient of the virus when infected cells die. δ_3 is the clearance rate of virus. The (1) model has been helpful in understanding HIV infection dynamics and developing specific treatment regimens [6, 7]. Based on this model, many mathematicians studied the dynamics of HIV infection in vivo [8–12].

Up until now, there has not been an effective way to cure HIV in the world, which implies that controlling the spread of the virus in vivo is very essential for us. It is well known that antibodies, one main component of the immune response, which are produced by B lymphocytes are used to identify and neutralize free virus particles in the blood. It then becomes a promising and effective therapy to reduce the virus in the blood in clinic experiments. In 2011, Balazs et al. [13] carried out a vectored immunoprophylaxis experiment to bring new hope to eradicating HIV. The experiment showed that the humanized mice receiving vectored immunoprophylaxis appeared to be fully protected from HIV infection. Based on this experiment, the authors in [14] presented their new model which was different from the previous one:

$$\begin{aligned}
\frac{dT}{dt} &= \Lambda - \delta_1 T - \beta_1 VT,\\
\frac{dI}{dt} &= \beta_1 VT - \delta_2 T^*,\\
\frac{dV}{dt} &= N\delta_2 T^* - \delta_3 V - \gamma_2 AV,\\
\frac{dA}{dt} &= \mu - \delta_5 A - \gamma VA.
\end{aligned} \tag{2}$$

Here, A is the concentration of antibodies in vivo. μ represents the neutralizing antibodies produced at a constant rate after the injection. δ_5 denotes the clearance rate of antibodies. $\gamma_2 AV$ represents the loss rate of the virus under the attack of antibodies. The term γAV depicts the loss of antibody from the effect of antibodies' involvement with the virus. Other parameters are the same with system (1).

Another main component of the immune response is cytotoxic T lymphocytes (CTLs), which are the T cells that are capable of recognizing and killing infected cells, and they would not be infected by HIV. Some papers were devoted to investigate the HIV models under the impacts of CTLs [8, 15–17], which indicates the CTLs have a critical role on the viral infection. Moreover, many researchers have taken into account the effect of both CTLs' response and antibodies [18–22] and the references therein. Specifically, in [20–22], the authors captured the main features of the complex interactions of HIV and immune responses and then formulated the impacts of immune responses as a term in the models instead of introducing a new variable. Their formulations make the mathematical analysis tractable. However, it cannot depict the dynamics of HIV under CTLs and antibodies in vivo exactly.

Therefore, to study the dynamics of HIV replication in vivo under CTLs and antibodies, we introduce two new variables into (1) to propose our model, which incorporates the CTLs into model (2):

$$\begin{aligned}
\frac{dT}{dt} &= \Lambda - \delta_1 T - \beta_1 VT,\\
\frac{dT^*}{dt} &= \beta_1 VT - \delta_2 T^* - \gamma_1 T^* C,\\
\frac{dV}{dt} &= N\delta_2 T^* - \delta_3 V - \gamma_2 AV - \beta_1 TV,\\
\frac{dC}{dt} &= \beta_2 T^* C - \delta_4 C,\\
\frac{dA}{dt} &= \mu - \delta_5 A - \gamma VA,
\end{aligned} \tag{3}$$

where C denotes the concentration of CTL cells, γ_1 represents the loss rate of infected cells under attack by CTLs, and δ_4 is the death rate of the CTL cells. The last term $\beta_1 VT$ in the third equation describes the loss rate of the virus because of entry into target cells. The term $\beta_2 T^* C$ represents the increment of CTL cells stimulated by infected T cells. All the other parameters in (3) are the same as those in (2).

We consider CTLs and antibodies as two major components of the immune response in our model (3), which describes HIV replication in vivo under the protection of the immune response. Compared to models that only consider CTLs or antibodies, the results are more informative. It can also be more accurate than those works in [20–22], where formulate the impacts of CTLs and antibodies as a term of the model. On the other hand, model (2) is proposed to investigate the viral dynamics for the introduction of vectored immunoprophylaxis antibodies in the experiment of [13]. As we mentioned before, our model (3) incorporates the CTLs into model (2), which can describe the dynamics of HIV under the CTLs in the vectored immunoprophylaxis experiment. It can provide the theoretical results for the impacts of CTLs in this experiment, which can be further extended to study the clinical possibilities of the experiment. Clearly, this model and its results cannot be derived from [18–22] and the references therein, where CTLs and antibodies are also considered in their models.

The organization of this paper is as follows: In the next section, we study the model (3). We study the well-posedness of solutions in Section 2. In Section 3, we study the existence of equilibria and then present the stability analysis of infection-free equilibrium in Section 4. We conduct the numerical simulation of this model in Section 5. A brief summary and discussion are shown in the last section.

2. Well-Posedness of Solutions

For the sake of brevity, we offer the following scaling:

$$\bar{t} = \delta_1 t,\ \bar{T} = \frac{\beta_1}{\delta_1} T,\ \bar{T}^* = \frac{\beta_2}{\delta_1} T^*,\ \bar{V} = \frac{\beta_1}{\delta_1} V,\ \bar{C} = \frac{\gamma_1}{\delta_1} C,$$
$$\bar{A} = \frac{\gamma_2}{\delta_1} A,\ \bar{\Lambda} = \frac{\Lambda\beta_1}{\delta_1^2},$$

$$\bar{\beta} = \frac{\beta_2}{\beta_1}, \bar{\delta}_1 = \frac{\beta_2}{\delta_1}, \bar{N} = \frac{N\delta_2\beta_1}{\delta_1\beta_2}, \bar{\delta}_2 = \frac{\delta_3}{\delta_1}, \bar{\delta}_3 = \frac{\delta 4}{\delta_1}, \bar{\mu} = \frac{\mu\gamma_2}{\delta_1^2}, \bar{\delta} 4 = \frac{\delta_5}{\delta_1}, \bar{\gamma} = \frac{\gamma}{\beta_1}. \tag{4}$$

Dropping the bars, model (3) becomes

$$\begin{cases} \dfrac{dT}{dt} = \Lambda - T - VT, \\ \dfrac{dT^*}{dt} = \beta VT - \delta_1 T^* - T^* C, \\ \dfrac{dV}{dt} = NT^* - \delta_2 V - AV - VT, \\ \dfrac{dC}{dt} = T^* C - \delta_3 C, \\ \dfrac{dA}{dt} = \mu - \delta_4 A - \gamma AV. \end{cases} \tag{5}$$

In this section, we show that all solutions of the system (5), for any given nonnegative initial conditions, are nonnegative.

Theorem 1. *Any solution of system (5), $(T(t), T^*(t), V(t), C(t), A(t))$, is nonnegative and ultimately bounded for $t > 0$ with any provided nonnegative initial conditions.*

Proof. . Firstly, we show that $T(t)$ is positive for $t > 0$. Assume that $t_1 > 0$ is the first time such that $T(t_1) = 0$. Then, according to the first equation of system (5), we have $dT/dt|_{t=t_1} = \Lambda > 0$, which implies that $T(t) \geq 0$ always holds for $t > 0$ with $T(0) > 0$. It is similar to show that $C(t) \geq 0$ and $A(t) > 0$ always hold true for $t > 0$ for any given positive initial conditions. □

To prove $V(t) \geq 0$ for $t > 0$, we argue it by contradiction. Let $t_2 > 0$ be the first time to make $V(t_2) = 0$, then we have $dV/dt|_{t=t_2} = NT^*(t_2)$. Solving $T^*(t)$ from the second equation of system (5) yields

$$T^*(t_2) = e^{-\int_0^{t_2}(\delta_1 + C(\varepsilon))d\varepsilon}\left(T^*(0) + \int_0^{t_2}\beta T(\theta)V(\theta)e^{\int_0^{\theta}(\delta_1 + C(\varepsilon))d\varepsilon}d\theta\right), \tag{6}$$

which means that $T^*(t_2) > 0$. Then we have $dV/dt|_{t=t_2} = NT^*(t_2) > 0$ and then $V(t) \geq 0$ for $t > 0$. Furthermore, we can also get

$$T^*(t) = e^{-\int_0^{t}(\delta_1 + C(\varepsilon))d\varepsilon}\left(T^*(0) + \int_0^{t}\beta T(\theta)V(\theta)e^{\int_0^{\theta}(\delta_1 + C(\varepsilon))d\varepsilon}d\theta\right) > 0. \tag{7}$$

It shows that $T^*(t)$ is nonnegative for $t > 0$.

Now we show that solutions of system (5) are ultimately uniformly bounded for $t > 0$. Firstly, from system (5), we have

$$\frac{dT(t)}{dt} \leq \Lambda - T, \frac{dA(t)}{dt} \leq \mu - \delta_4 A(t), \tag{8}$$

which means that $\limsup_{t\longrightarrow\infty} T(t) \leq \Lambda$ and $\limsup_{t\longrightarrow\infty} A(t) \leq \mu/\delta_4$. Adding the former two equations yields

$$\frac{d(\beta T(t) + T^*(t))}{dt} \leq \beta\Lambda - d_1(\beta T(t) + T^*(t)), \tag{9}$$

where $d_1 = \min\{\beta, \delta_1\}$, which means that $\limsup_{t\longrightarrow\infty} (\beta T(t) + T^*(t)) \leq \beta\Lambda/d_1$. It follows that

$$\frac{dV(t)}{dt} \leq \frac{N\beta\Lambda}{d_1} - \delta_2 V(t), \tag{10}$$

and then $\limsup_{t\longrightarrow\infty} V(t) \leq N\beta\Lambda/d_1\delta_2$. Therefore, we obtain that

$$\frac{d(T^*(t) + C(t))}{dt} \leq \frac{N\beta^2\Lambda^2}{d_1\delta_2} - d_2(T^*(t) + C(t)), \tag{11}$$

where $d_2 = \min\{\delta_1, \delta_3\}$, which means that $\limsup_{t\longrightarrow\infty}(T^*(t) + C(t)) \leq N\beta^2\Lambda^2/d_1d_2\delta_2$.

Therefore, we get the following feasible region:

$$\Gamma = \left\{(T, T^*, V, C, A) \in \mathbb{R}_+^5 : 0 < T(t) \leq \Lambda, 0 < \beta T(t) + T^*(t) \leq \frac{\beta\Lambda}{d_1}, 0 \leq V(t) \leq \frac{N\beta\Lambda}{d_1\delta_2}, 0 \leq T^*(t) + C(t) \leq \frac{N\beta^2\Lambda^2}{d_1d_2\delta_2}, 0 < A(t) \leq \frac{\mu}{\delta_4}\right\}. \tag{12}$$

It can be verified that Γ is positively invariant with respect to system (5).

3. The Existence of Equilibria

It is easy to obtain that the infection-free equilibrium (IFE) is $E_0 = (\Lambda, 0, 0, 0, \mu/\delta_4)$. In virus dynamics, the basic reproduction number is a basic concept, which denotes the expected number of secondary cases produced, in a completely susceptible population, by a typical infective individual [23]. Obviously, whether the basic reproduction number exceeds unit one is an important factor to determine the spread or extinction of the infection, biologically. Hence, it is necessary and reasonable for us to derive the basic reproduction number of model (5). By the method introduced in [23], we rewrite (5) as $dx/dt = \mathscr{F} - \mathscr{V}$, where $x = (T, T^*, V, C, A)^T$.

$$\mathscr{F} = \begin{pmatrix} \Lambda \\ \beta VT \\ NT^* \\ 0 \\ \mu \end{pmatrix}, \mathscr{V} = \begin{pmatrix} T + VT \\ \delta_1 T^* + T^* C \\ \delta_2 V + AV + VT \\ -T^* C + \delta_3 C \\ \delta_4 A + \gamma AV \end{pmatrix}. \tag{13}$$

By computing $R_0 = \rho(\mathfrak{F}\mathfrak{V}^{-1})$, where $\rho(B)$ denotes the spectral radius of a matrix B

$$\mathfrak{F} = \begin{pmatrix} 0 & 0 & 0 & 0 & 0 \\ 0 & 0 & \beta\Lambda & 0 & 0 \\ 0 & N & 0 & 0 & 0 \\ 0 & 0 & 0 & 0 & 0 \\ 0 & 0 & 0 & 0 & 0 \end{pmatrix},$$

$$\mathfrak{V} = \begin{pmatrix} 1 & 0 & T & 0 & 0 \\ 0 & \delta_1 & 0 & 0 & 0 \\ 0 & 0 & \delta_2 + \Lambda + \dfrac{\mu}{\delta_4} & 0 & 0 \\ 0 & 0 & 0 & \delta_3 & 0 \\ 0 & 0 & 0 & 0 & \delta_4 \end{pmatrix}, \tag{14}$$

we can obtain that the basic reproduction number of virus in (5) is

$$R_0 = \sqrt{\frac{N\beta\Lambda}{\delta_1(\delta_2 + \Lambda + \mu/\delta_4)}}. \tag{15}$$

3.1. The Existence of the Immune-Free Infection Equilibrium. It is obvious that model (5) has an immune-free infection equilibrium $\tilde{E} = (\tilde{T}, \tilde{T}^*, \tilde{V}, 0, \tilde{A})$. It is clear that the existence of this immune-free infection equilibrium is equivalent to study the existence of the infection equilibrium of the following system:

$$\begin{cases} \dfrac{dT}{dt} = \Lambda - T - VT, \\ \dfrac{dT^*}{dt} = \beta VT - \delta_1 T^*, \\ \dfrac{dV}{dt} = NT^* - \delta_2 V - AV - VT, \\ \dfrac{dA}{dt} = \mu - \delta_4 A - \gamma AV. \end{cases} \tag{16}$$

Then, we study the existence of infection equilibrium of system (16). An infection equilibrium $\tilde{E} = (\tilde{T}, \tilde{T}^*, \tilde{V}, \tilde{A})$ satisfies

$$\begin{cases} \Lambda - \tilde{T} - \tilde{V}\tilde{T} = 0, \\ \beta\tilde{V}\tilde{T} - \delta_1 \tilde{T}^* = 0, \\ N\tilde{T}^* - \delta_2 \tilde{V} - \tilde{A}\tilde{V} - \tilde{V}\tilde{T} = 0, \\ \mu - \delta_4 \tilde{A} - \gamma\tilde{A}\tilde{V} = 0. \end{cases} \tag{17}$$

Obviously, we have

$$\tilde{T} = \frac{\Lambda}{1 + \tilde{V}}, \tilde{T}^* = \frac{\beta\tilde{V}}{\delta_1}\tilde{T}, \tilde{A} = \frac{\mu}{\delta_4 + \gamma\tilde{V}}, \tag{18}$$

where $\tilde{V}$ satisfies the equation

$$f(\tilde{V}) = M_1\tilde{V}^2 + M_2\tilde{V} + M_3 = 0, \tag{19}$$

in which

$$\begin{aligned} M_1 &= \delta_2\delta_4\gamma > 0, \\ M_2 &= \delta_4(\delta_2\delta_4 + \mu) - \delta_4\gamma(\Lambda + \delta_2)\left(R_0^2 - 1\right) - \gamma\mu R_0^2, \\ M_3 &= \delta_4((\Lambda + \delta_2)\delta_4 + \mu)\left(1 - R_0^2\right). \end{aligned} \tag{20}$$

From M_3, we know that system (16) has a unique infection equilibrium $\tilde{E}_2 = (T_2, T_2^*, V_2, A_2)$, when $R_0 > 1$, where

$$\begin{aligned} &V_2 = \frac{-M_2 + \sqrt{\Delta}}{2M_1}, T_2 = \frac{\Lambda}{1 + V_2}, T_2^* = \frac{\beta V_2}{\delta_1}T_2, \\ &A_2 = \frac{\mu}{\delta_4 + \gamma V_2}, \Delta = M_2^2 - 4M_1M_3. \end{aligned} \tag{21}$$

As in the case of $R_0 < 1$, note that

$$\begin{aligned} m_1 &= \gamma^2((\delta_2 + \Lambda)\delta_4 + \mu)^2 > 0, \\ m_2 &= -2((\delta_2 + \Lambda)\delta_4 + \mu)((\delta_2 + \Lambda)\gamma + \mu - \delta_2\delta_4)\delta_4\gamma, \\ m_3 &= \left(((\gamma - \delta_4)\delta_2 + \Lambda\gamma - \mu)^2 + 4\Lambda\gamma\mu\right)\delta_4^2 > 0, \\ R_0^c &= \frac{-m_2 + \sqrt{m_2^2 - 4m_1m_3}}{2m_1}. \end{aligned} \tag{22}$$

We define that

$$V_1 = \frac{-M_2 - \sqrt{\Delta}}{2M_1}, T_1 = \frac{\Lambda}{1 + V_1}, T_1^* = \frac{\beta V_1}{\delta_1} T_1, A_1 = \frac{\mu}{\delta_4 + \gamma V_1}. \tag{23}$$

Theorem 2. *System (16) has an infection equilibria $\tilde{E}_2 = (T_2, T_2^*, V_2, A_2)$ if $R_0 > 1$. Hence, system (5) admits an immune-free equilibria $E_2 = (T_2, T_2^*, V_2, 0, A_2)$ if $R_0 > 1$.*

Lemma 3. *Let $\mu + \delta_2\delta_4 < \mu\gamma/\delta_4$ and $R_0 < 1$ hold. We have the following conclusions:*

(1) System (16) has two infection equilibria $\tilde{E}_1 = (T_1, T_1^*, V_1, A_1)$ and $\tilde{E}_2 = (T_2, T_2^*, V_2, A_2)$ when $\sqrt{R_0^c} < R_0 < 1$

(2) System (16) has a unique infection equilibrium $\tilde{E}_1 = \tilde{E}_2$ when $R_0 = \sqrt{R_0^c}$

(3) System (16) has no infection equilibrium when $R_0 < \sqrt{R_0^c}$

Proof. Clearly, (19) has no positive root when $M_2 > 0$, two positive roots when $M_2 < 0$ and $\Delta > 0$, has a positive root when $M_2 < 0$ and $\Delta = 0$, and no positive root when $\Delta < 0$. So, we study the case that $M_2 < 0$.

To determine the signs of Δ in terms of the basic reproduction number, we denote R_0^2 by R_1 so that

$$N = \frac{\delta_1(\delta_2\delta_4 + \delta_4\Lambda + \mu)}{\beta\Lambda\delta_4} R_1. \tag{24}$$

It is easy to obtain

$$\Delta = m_1R_1^2 + m_2R_1 + m_3, \tag{25}$$

where $m_i (i = 1, 2, 3)$ are given in (22). Since $M_2 < 0$, we get

$$R_1 > \frac{(\mu + \delta_2\delta_4 + \delta_2\gamma + \Lambda\gamma)\delta_4}{\gamma(\delta_2\delta_4 + \Lambda\delta_4 + \mu)} := R_2. \tag{26}$$

Suppose

$$\mu + \delta_2\delta_4 < \frac{\mu\gamma}{\delta_4}, \tag{27}$$

then $R_2 < 1$. Let $h(x) = m_1x^2 + m_2x + m_3$; then we have

$$\begin{aligned} h(R_2) &= m_1^2R_2^2 + m_2R_2 + m_3 = 4\delta_2\delta_4^3\left(\delta_2\delta_4 + \mu - \frac{\mu\gamma}{\delta_4}\right) < 0, \\ h(1) &= m_1 + m_2 + m_3 = \left((\gamma - \delta_4)\mu - \delta_2\delta_4^2\right)^2 > 0. \end{aligned} \tag{28}$$

If $\mu + \delta_2\delta_4 < \mu\gamma/\delta_4$, we can get $\gamma > \delta_4$, and then

$$\Delta_1 = m_2^2 - 4m_1m_3 = 16(\gamma - \delta_4)((\Lambda + \delta_2)\delta_4 + \mu)^2\gamma^2\delta_2\delta_4^2\mu > 0. \tag{29}$$

It follows that $h(x) = 0$ admits a root R_0^c, which is defined in (22), in interval $(R_2, 1)$. Clearly, we have $\Delta = 0$ when $R_0 = \sqrt{R_0^c}$; $\Delta > 0$ when $\sqrt{R_0^c} < R_0$ and $\Delta < 0$ when $0 < R_0 < \sqrt{R_0^c}$.

According to Lemma 3, we can conclude the following theorem. □

Theorem 4. *Let $\mu + \delta_2\delta_4 < \mu\gamma/\delta_4$ and $R_0 < 1$ hold.*

(1) System (5) has two immune-free equilibria $E_1 = (T_1, T_1^*, V_1, 0, A_1)$ and $E_2 = (T_2, T_2^*, V_2, 0, A_2)$ when $\sqrt{R_0^c} < R_0 < 1$

(2) System (5) has a unique immune-free equilibrium when $R_0 = \sqrt{R_0^c}$

(3) System (5) has no immune-free equilibrium when $R_0 < \sqrt{R_0^c}$

3.2. The Existence of the Immune-Present Infection Equilibrium of System (5). An immune-present infection equilibrium $\bar{E} = (\bar{T}, \bar{T}^*, \bar{V}, \bar{C}, \bar{A})$ satisfies

$$\begin{cases} \Lambda - \bar{T} - \bar{V}\bar{T} = 0, \\ \beta\bar{V}\bar{T} - \delta_1\bar{T}^* - \bar{T}^*\bar{C} = 0, \\ N\bar{T}^* - \delta_2\bar{V} - \bar{A}\bar{V} - \bar{V}\bar{T} = 0, \\ \bar{T}^*\bar{C} - \delta_3\bar{C} = 0, \\ \mu - \delta_4\bar{A} - \gamma\bar{A}\bar{V} = 0. \end{cases} \tag{30}$$

Direct computation leads to

$$\bar{T} = \frac{\Lambda}{1 + \bar{V}}, \bar{T}^* = \delta_3, \bar{C} = \frac{\beta\Lambda\bar{V}}{\delta_3(1 + \bar{V})} - \delta_1, \bar{A} = \frac{\mu}{\delta_4 + \gamma\bar{V}}, \tag{31}$$

where $\bar{V}$ satisfies the equation

$$g(\bar{V}) = a_1\bar{V}^3 + a_2\bar{V}^2 + a_3\bar{V} + a_4, \tag{32}$$

in which

$$
\begin{aligned}
a_1 &= \delta_2\gamma > 0,\\
a_2 &= \mu + \delta_2\delta_4 + \delta_2\gamma + \Lambda\gamma - N\delta_3\gamma\\
&= \frac{\delta_2\delta_4\gamma(2-R^*) + \delta_4\gamma\Lambda(1-R^*) + \mu\gamma(1-R^*) + \delta_2^2\delta_4^2 + \delta_2\gamma^2 + \Lambda\gamma^2 + \mu\delta_4}{\delta_4+\gamma},\\
a_3 &= \mu + \delta_2\delta_4 + \delta_4\Lambda - N\delta_3\gamma - N\delta_3\delta_4\\
&= (\mu + \delta_2\delta_4 + \delta_4\Lambda)(1-R^*),\\
a_4 &= -N\delta_3\delta_4 < 0,\\
R^* &= \frac{N\delta_3(\delta_4+\gamma)}{\delta_2\delta_4 + \mu + \Lambda\delta_4}.
\end{aligned}
\tag{33}
$$

To ensure the existence of a positive equilibrium, we let $\beta\Lambda - \delta_1\delta_3 > 0$ and $\bar{C} > 0$, which is equivalent to

$$
\bar{V} > \frac{\delta_1\delta_3}{\beta\Lambda - \delta_1\delta_3}. \tag{34}
$$

By the mathematical analysis, we know that $g(x) = a_1x^3 + a_2x^2 + a_3x + a_4 = 0$ must have a unique positive solution when $a_3 < 0 (R^* > 1)$. When $a_3 \geq 0 (R^* \leq 1)$, it is easy to get $a_2 > 0$. Then $g(x) = 0$ has also a unique positive solution when $a_3 \geq 0$. Therefore, we have the following theorem.

Theorem 5. *System (5) has a unique immune-present infection equilibrium $E_3 = (T_3, T_3^*, V_3, C_3, A_3)$ when $V_3 > \delta_1\delta_3/(\beta\Lambda - \delta_1\delta_3)$, where V_3 is the positive solution of $g(\bar{V}) = 0$. Otherwise, system (5) has no immune-present infection equilibrium.*

4. The Stability of Equilibra

The Jacobian matrix of (5) at an equilibrium $E = (T, T^*, V, C, A)$ is

$$
J(E) = \begin{bmatrix}
-V-1 & 0 & -T & 0 & 0\\
V\beta & -C-\delta_1 & \beta T & -T^* & 0\\
-V & N & -A-T-\delta_2 & 0 & -V\\
0 & C & 0 & T^*-\delta_3 & 0\\
0 & 0 & -\gamma A & 0 & -V\gamma - \delta_4
\end{bmatrix}. \tag{35}
$$

Theorem 6. *The infection-free equilibrium E_0 is asymptotically stable if $R_0 < 1$ and is unstable if $R_0 > 1$. The immune-free equilibrium E_1 is unstable when it exists.*

Proof. The characteristic equation of the Jacobian matrix of (5) at E_0, $J(E_0)$, in λ is

$$
\begin{aligned}
&(\lambda+1)(\lambda+\delta_3)(\lambda+\delta_4)\left(\lambda^2 + \left(\delta_1 + \delta_2 + \frac{\mu}{\delta_4} + \Lambda\right)\lambda\right.\\
&\left. + \delta_1\left(\delta_2 + \Lambda + \frac{\mu}{\delta_4}\right)\left(1 - R_0^2\right)\right) = 0.
\end{aligned}
\tag{36}
$$

It follows that all the characteristic roots have negative real parts when $R_0 < 1$, and one characteristic root is positive when $R_0 > 1$. Thus, we know that E_0 is asymptotically stable when $R_0 < 1$ and is unstable when $R_0 > 1$.

The characteristic polynomial of $J(E_1)$ in λ is then

$$
F_1(\lambda) = (\lambda + \delta_3 - T_1^*)\left(\lambda^4 + c_3\lambda^3 + c_2\lambda^2 + c_1\lambda + c_0\right), \tag{37}
$$

where

$$
\begin{aligned}
c_3 &= \delta_1 + (1+\gamma)V_1 + \delta_2 + A_1 + T_1 + \delta_4 + 1 > 0,\\
c_2 &= \gamma V_1^2 + ((1+\gamma)(\delta_1+\delta_2) + \gamma(1+T_1) + A_1 + \delta_4)V_1\\
&\quad + (\delta_1 + \delta_2 + A_1 + T_1)(1+\delta_4) + \delta_4 > 0,\\
c_1 &= \delta_1(\delta_2 + \delta_4 + A_1) + (\delta_1+\delta_2)\gamma + (\delta_2 + A_1)\delta_4 - \delta_1\gamma A_1,\\
c_0 &= \delta_1 V_1((\delta_4 - \gamma)A_1 + \delta_2(\delta_4 + \gamma V_1)).
\end{aligned}
\tag{38}
$$

We note that

$$
\begin{aligned}
c_0 &= \frac{\delta_1 V_1}{\delta_4 + \gamma V_1}\left(2M_1V_1 + M_2 - \frac{\gamma}{\delta_4}(M_2V_1 + 2M_3)\right)\\
&= -\sqrt{\Delta}\left(\frac{\gamma}{\delta_4}V_1 + 1\right) < 0.
\end{aligned}
\tag{39}
$$

It then implies that $J(E_1)$ has at least a positive real eigenvalue, which means that E_1 is unstable.

As for the stability of E_2, we can also obtain that the characteristic polynomial of $J(E_2)$ in λ is then

$$
F_2(\lambda) = (\lambda + \delta_3 - T_2^*)\left(\lambda^4 + \hat{c}_3\lambda^3 + \hat{c}_2\lambda^2 + \hat{c}_1\lambda + \hat{c}_0\right), \tag{40}
$$

where

$$
\begin{aligned}
\hat{c}_3 &= \delta_1 + (1+\gamma)V_2 + \delta_2 + A_2 + T_2 + \delta_4 + 1 > 0,\\
\hat{c}_2 &= \gamma V_2^2 + ((1+\gamma)(\delta_1+\delta_2) + \gamma(1+T_2) + A_2 + \delta_4)V_2\\
&\quad + (\delta_1 + \delta_2 + A_2 + T_2)(1+\delta_4) + \delta_4 > 0,\\
\hat{c}_1 &= \delta_1(\delta_2 + \delta_4 + A_2) + (\delta_1+\delta_2)\gamma + (\delta_2 + A_2)\delta_4 - \delta_1\gamma A_2,\\
\hat{c}_0 &= \delta_1 V_2((\delta_4 - \gamma)A_2 + \delta_2(\delta_4 + \gamma V_2)).
\end{aligned}
\tag{41}
$$

□

Hence, according to Routh-Hurwitz criterion, we obtain the following theorem.

Theorem 7. *When system (5) admits the immune-free equilibrium E_2, it is locally stable when $T_2^* < \delta_3$, $\hat{c}_1 > 0$, $\hat{c}_0 > 0$, $\hat{c}_3\hat{c}_2 > \hat{c}_1$, and $\hat{c}_1\hat{c}_2\hat{c}_3 > \hat{c}_1^2 + \hat{c}_3^2\hat{c}_0$.*

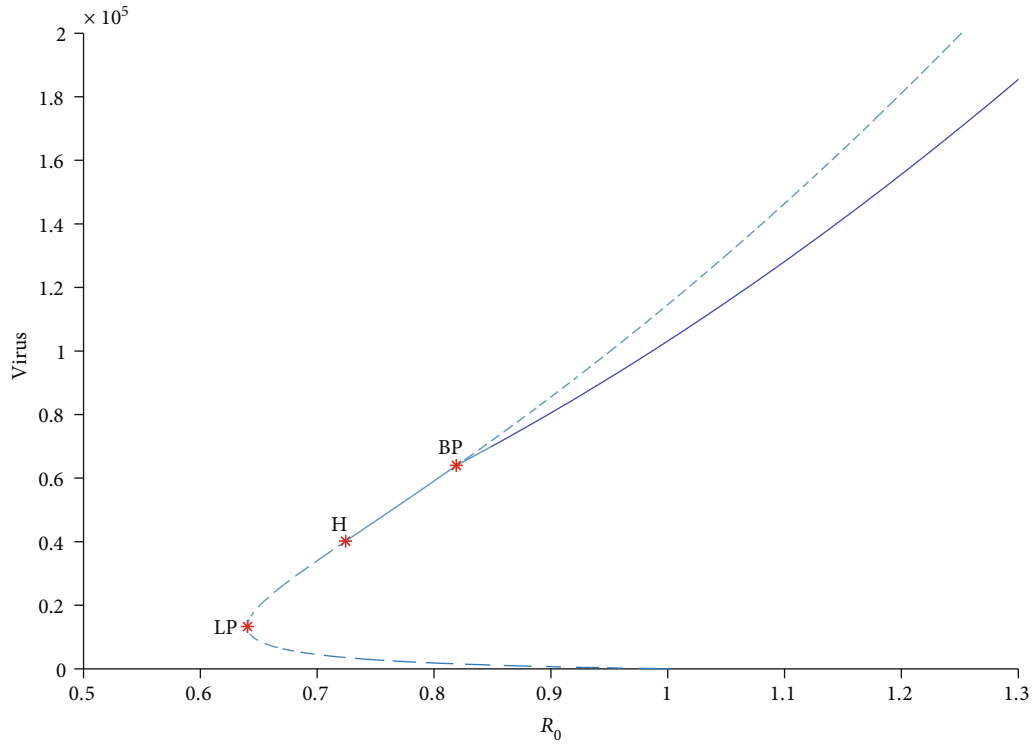

Figure 1: Two immune-free infection equilibria and an immune-present infection equilibrium coexist. The dashed (solid) curve represents an unstable (stable) equilibrium. LP is a limit point, H represents a Hopf point, and BP represents a branch point.

Obviously, the characteristic polynomial of $J(E_3)$ in λ is then

$$F_3(\lambda) = \lambda^5 + \bar{c}_4\lambda^4 + \bar{c}_3\lambda^3 + \bar{c}_2\lambda^2 + \bar{c}_1\lambda + \bar{c}_0, \tag{42}$$

where

$$\begin{aligned}
\bar{c}_4 &= \delta_1 + (1+\gamma)V_3 + \delta_2 + A_3 + T_3 + \delta_4 + 1 + C_3 > 0,\\
\bar{c}_3 &= ((1+\gamma)V_3 + 1 + \delta_3 + \delta_4)C_3 + \gamma V_3^2\\
&\quad + (\delta_1 + \delta_2 + \delta_4 + A_3 + \gamma(1 + \delta_1 + \delta_2 + T_3))V_3\\
&\quad + (\delta_1 + \delta_2 + A_3 + T_3)(1 + \delta_4) + \delta_4 > 0,\\
\bar{c}_2 &= (\delta_1 + \delta_2 + C_3)\gamma V_3^2 + (\delta_2 + \delta_3 + \delta_4 + \gamma + \delta_3\gamma + A_3)V_3C_3\\
&\quad + ((1+\delta_3)\delta_4 + (1 + \delta_2 + A_3 + T_3)\delta_3)C_3\\
&\quad + ((\delta_2 + A_3)\delta_4 + (\delta_2 + \delta_4 + \gamma + A_3 - \gamma A_3)\delta_1\\
&\quad + (\delta_2 + T_3 - A_3C_3)\gamma)V_3 + (\delta_1 + \delta_2 + A_3 + T_3)\delta_4,\\
\bar{c}_1 &= (\delta_1\delta_2 + (\delta_2 + \delta_3)C_3)\gamma V_3^2 + ((\delta_1 + C_3)(\delta_2 + A_3)\delta_4\\
&\quad + (\delta_2 + \delta_3A_3 + \delta_4 + \gamma(1 + \delta_2 + T_3))\delta_3C_3)V_3\\
&\quad + (\delta_4 + (1+\delta_4)(\delta_2 + A_3 + T_3))\delta_3C_3 > 0,\\
\bar{c}_0 &= \delta_3C_3(\delta_2\gamma V_3^2 + ((\delta_2 + A_3)\delta_4 + (\delta_2 + T_3)\gamma)V_3\\
&\quad + (\delta_1 + A_3 + T_3)\delta_4) > 0.
\end{aligned} \tag{43}$$

According to Routh-Hurwitz criterion, we can also obtain the following theorem.

Theorem 8. *When system (5) admits the immune-present equilibrium E_3, it is locally stable when $\bar{c}_2 > 0$, $\bar{c}_3\bar{c}_4 - \bar{c}_2 > 0$, $\bar{c}_2\bar{c}_3\bar{c}_4 + \bar{c}_0\bar{c}_4 - \bar{c}_2^2 - \bar{c}_1\bar{c}_4^2 > 0$, and $\bar{c}_1(\bar{c}_4(\bar{c}_2\bar{c}_3 - \bar{c}_1\bar{c}_4) - \bar{c}_2^2) + \bar{c}_0(2\bar{c}_1\bar{c}_4 + \bar{c}_2\bar{c}_3 - \bar{c}_3^2\bar{c}_4 - \bar{c}_0) > 0$.*

5. Bifurcations and Numerical Simulation

In this section, we study bifurcations of model (3) on the basis of Section 3 and Section 4. When R_0 crosses unit one, the IFE E_0 loses stability, which results in a bifurcation where a curve of endemic equilibria emerges. The bifurcation is forward if the endemic curve occurs when R_0 is slightly larger than one, and there is no positive equilibrium near the E_0 for $R_0 < 1$. In contrast, the bifurcation is backward if a positive equilibrium occurs when $R_0 < 1$. Now, we derive the condition for the backward bifurcation from E_0 of model (3). Notice that Theorem 4 implies that (24) is the existent condition of the backward bifurcation of model (5). By (4), we get an equivalent equation of (27):

$$B_1 := \frac{\mu\gamma\gamma_2}{\delta_5^2} - \frac{\delta_3\beta_1}{\delta_1} - \frac{\mu\beta_1\gamma_2}{\delta_1\delta_5} > 0. \tag{44}$$

Thus, we show the proposition below.

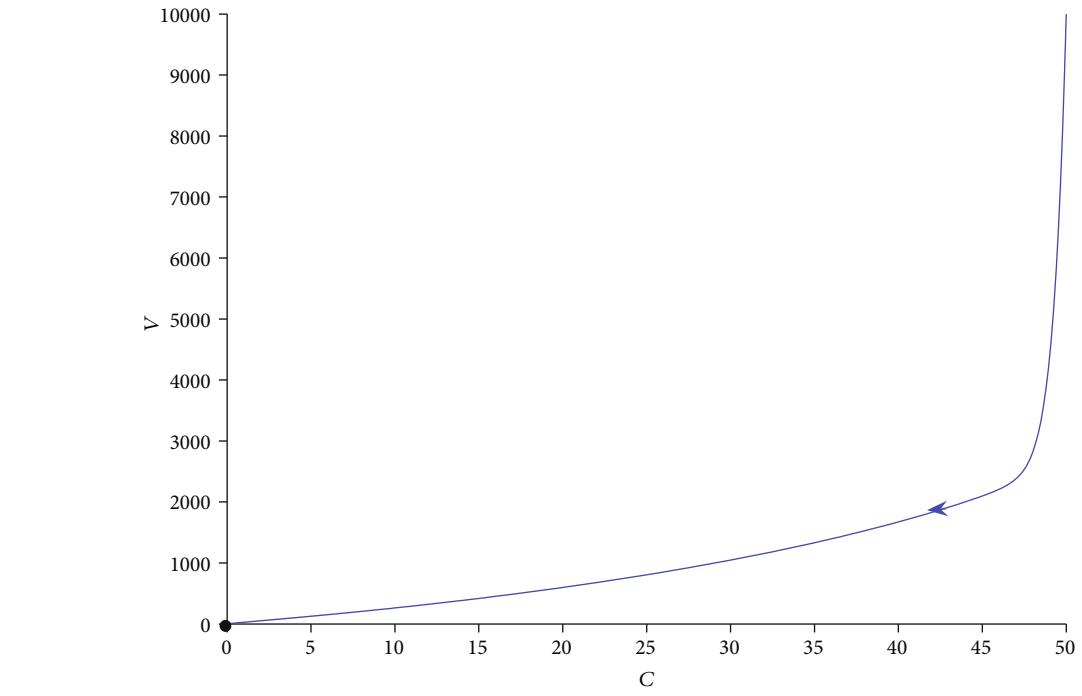

(a)

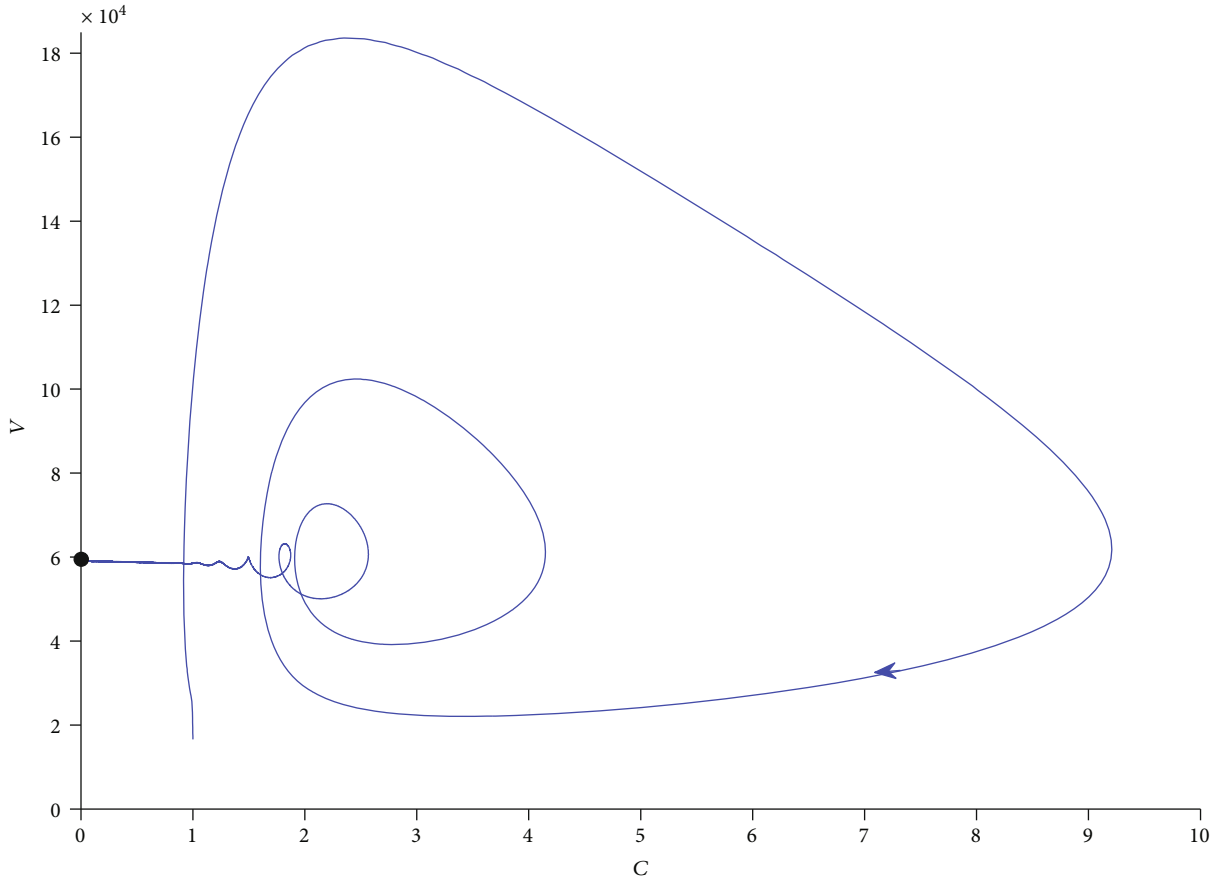

(b)

Figure 2: (a) A numerical solution of model (3) from (4000,30,10000,20,50) tends to an infection-free equilibrium as time tends to infinity when $R_0 = 0.8$. (b) A numerical solution of model (3) from (6140,635,16572,538,1) tends to an immune-free infection equilibrium as time tends to infinity when $R_0 = 0.8$.

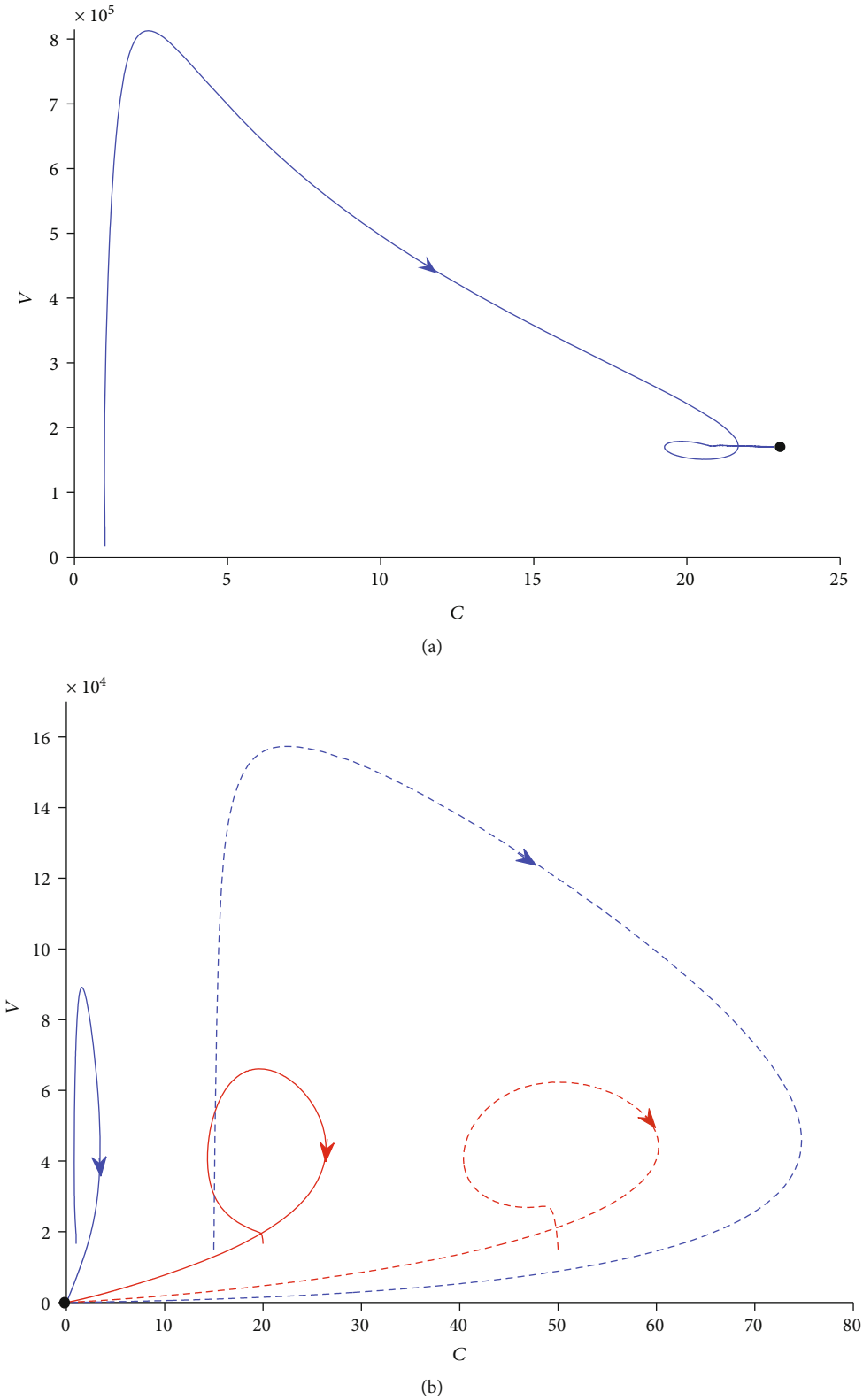

Figure 3: (a) A numerical solution of model (3) from (6140,635,16572,538,1) tends to an immune-present infection equilibrium as time tends to infinity when $R_0 = 1.25$. (b) Numerical solutions of model (3) tend to the infection-free equilibrium as time tends to infinity with the different initial values when $R_0 = 0.7$.

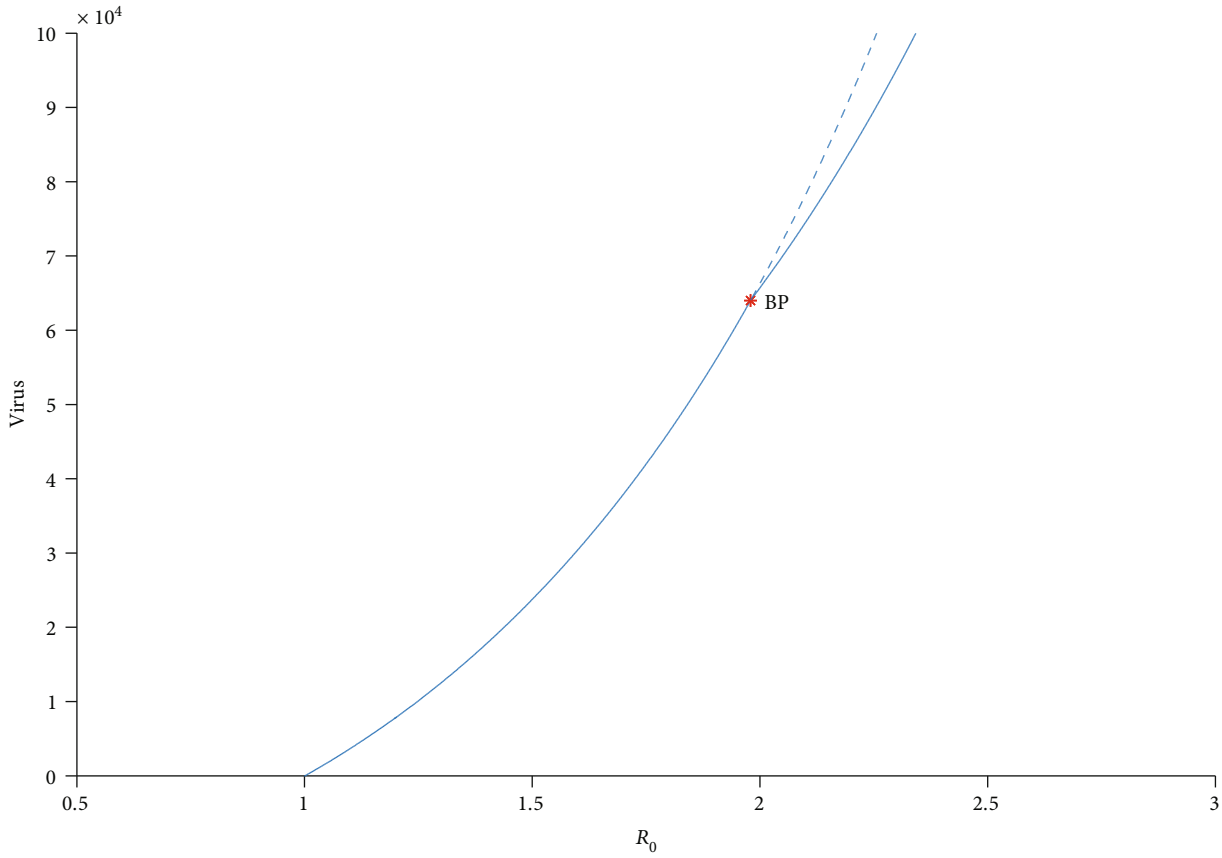

FIGURE 4: A immune-free infection equilibrium and an immune-present infection equilibrium coexist when $R_0 > 1$. The dashed (solid) curve represents an unstable (stable) equilibrium. BP represents a branch point.

Proposition 9. *System (3) admits a backward bifurcation as R_0 crosses unity if $B_1 > 0$ and admits a forward bifurcation if $B_1 < 0$.*

In this section, we implement numerical simulations on the basis of the MatCont package [24, 25] to testify the theoretical results above and explore more patterns of dynamical behaviors of model (3). We select $\Lambda = 100$, $\delta_1 = 0.008$, $\delta_2 = 0.08$, $\delta_3 = 3$, $\delta_4 = 0.05$, $\delta_5 = 0.02$, $\beta_1 = 5 \times 10^{-7}$, $\beta_2 = 5 \times 10^{-5}$, $\gamma_1 = 0.0005$, $\gamma_2 = 0.005$, and $\mu = 100$ from [8, 14].

If $\gamma = 10^{-5}$, we have $B_1 = 0.01075 > 0$ and a backward bifurcation exists from Proposition 9. We derive a bifurcation figure shown in Figure 1. To further address the results of Figure 1 at length, we get evolutionary results, as presented by Figures 2 and 3.

From Figure 1, we find a Hopf bifurcation point (H) at $R_0 = 0.724$, a fold bifurcation point (LP) at $R_0 = 0.6404$, and a branch point (BP) at $R_0 = 0.819$. It illustrates that two unstable immune-free infection equilibria coexist with a stable infection-free equilibrium when $0.6404 < R_0 < 0.724$; a stable immune-free infection equilibrium, an unstable immune-free infection equilibrium, and a stable infection-free equilibrium coexist when $0.724 < R_0 < 0.819$ (see Figure 2); and an unstable immune-free infection equilibrium coexists with a stable immune-present infection equilibrium when $R_0 > 0.819$ (see Figure 3(a)). Further numerical simulations indicate that any solution tends to an infection-free equilibrium when $R_0 < 0.724$ (see Figure 3(b)), which means that the subthreshold 0.724 of R_0 is required to eliminate the infection. It is different to the classical backward bifurcation that needs $R_0 < 0.6404$ to eliminate the infection.

When $\gamma = 10^{-7}$, we have $B_1 = -0.001625 < 0$, and a forward bifurcation exists from Proposition 9. When we get a bifurcation figure shown in Figure 4, the detailed evolutionary processes are, correspondingly, illustrated in Figure 5.

From Figure 4, a branch point (BP) is observed at $R_0 = 1.979166$. It demonstrates a stable infection-free equilibrium exists when $R_0 < 1$; a stable immune-free infection equilibrium, and an unstable infection-free equilibrium coexist when $1 < R_0 < 1.979166$ (see Figure 5(a)), and an unstable immune-free infection equilibrium coexists with a stable immune-present infection equilibrium when $R_0 > 1.979166$ (see Figure 5(b)).

Note that the qualitative difference between Figures 1 and 4 results from the fact that the value of γ in Figure 1 is higher than it is in Figure 4. This indicates that a stronger loss of antibodies' involvement with a virus can lead to a backward bifurcation, which supports the result of Proposition 9.

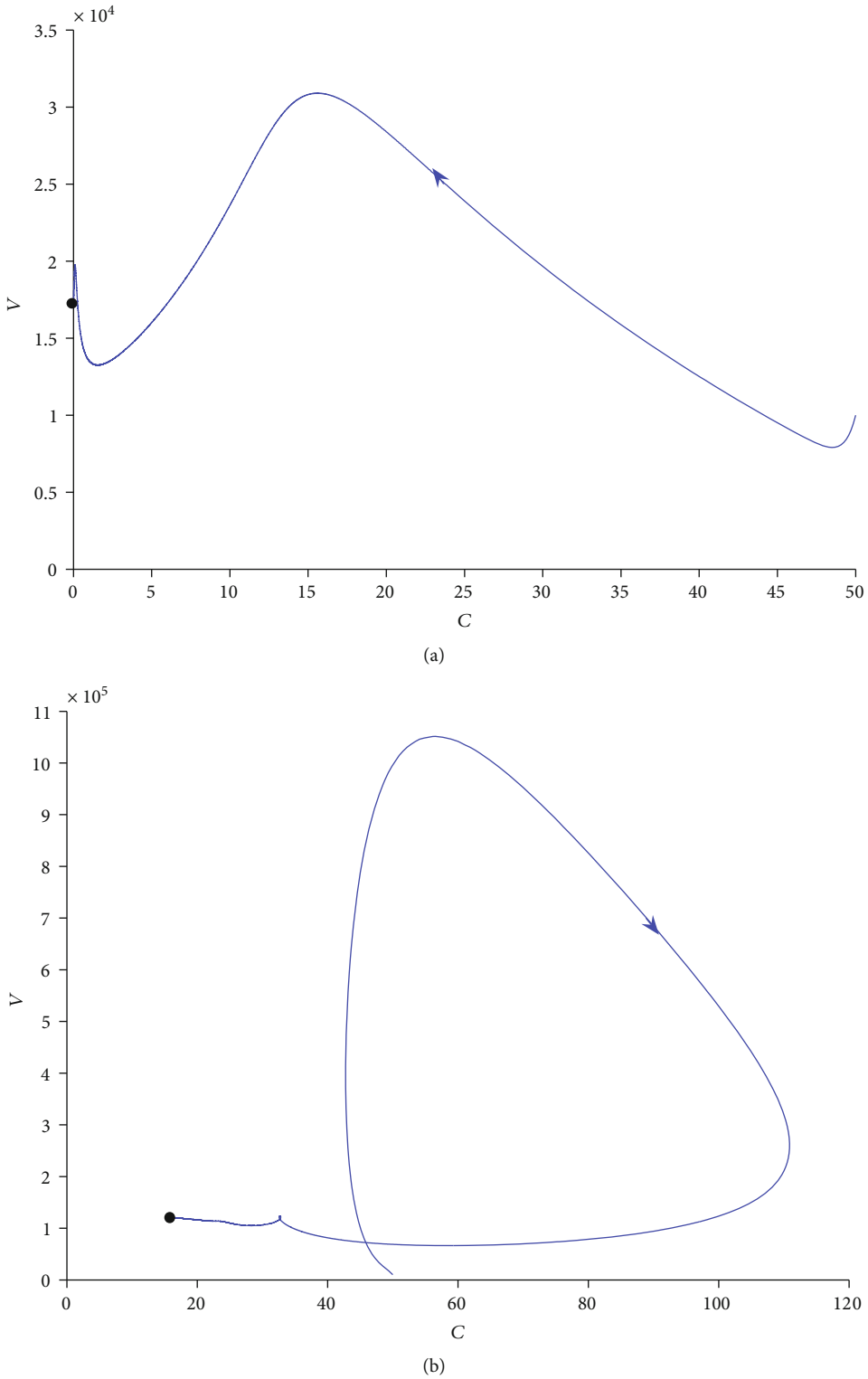

FIGURE 5: For two cases, $R_0 = 1.4$ and $R_0 = 2.5$, a numerical solution of model (3) from (4000,30,10000,20,50) tends to an immune-free infection equilibria and the immune-present infection equilibrium as time tends to infinity, respectively.

6. Conclusion and Discussion

In this paper, we focused on the modeling analysis of HIV epidemics, which incorporated immune systems based on CTLs and vectored immunoprophylaxis for controlling HIV replication. To address this role of immune response in detail, we integrated the immune response as a term into the model (3).

Specifically, we gave the analytical condition of the existence of equilibria. We further studied the local stability of

the existing equilibria. According to these theoretical results, we described the bifurcation figures of the given model. We noted that there exists a backward bifurcation at the infection-free equilibrium, thereby, demonstrating that driving the basic reproduction number (R_0) below 1 is not enough to eliminate HIV. More significantly, we observed a Hopf point at $R_0 = 0.724$, which indicates the classical strategy to drive R_0 below a certain value (limit point) 0.6404 maybe unnecessary. Due to these findings, we noted that it is feasible to extinguish the infection even when R_0 is below 0.724. Meanwhile, a forward bifurcation and an immune-present infection equilibrium exist in this model. Therefore, any strategy to drive R_0 below 1 is adequate to clear the infection away, according to our results.

Using numerical simulations and mathematical analyses of the proposed model, we can gain insights into the mechanisms of viral infection under the conditions of vectored immunoprophylaxis and immune response. With the introduction of the immune response, the model exhibits rich dynamical characteristics. As a result of the above findings, vectored immunoprophylaxis may be an effective therapy for HIV, and immune responses have a great influence on viral infection in vivo, which is overlooked in [14].

Data Availability

No data were used to support this study.

Conflicts of Interest

The authors declare that they have no conflicts of interest.

Acknowledgments

We are very grateful to all the referees for careful reading and valuable comments which led to important improvements of our original manuscript.

References

[1] P. K. Tiwari, R. K. Rai, S. Khajanchi, R. K. Gupta, and A. K. Misra, "Dynamics of coronavirus pandemic: effects of community awareness and global information campaigns," *The European Physical Journal Plus*, vol. 136, no. 10, p. 994, 2021.

[2] S. Khajanchi, K. Sarkar, J. Mondal, K. S. Nisar, and S. F. Abdelwahab, "Mathematical modeling of the COVID-19 pandemic with intervention strategies," *Results in Physics*, vol. 25, p. 104285, 2021.

[3] R. K. Rai, S. Khajanchi, P. K. Tiwari, E. Venturino, and A. K. Misra, "Impact of social media advertisements on the transmission dynamics of COVID-19 pandemic in India," *Journal of Applied Mathematics and Computing*, vol. 68, no. 1, pp. 19–44, 2022.

[4] M. A. Nowak and C. R. Bangham, "Population dynamics of immune responses to persistent viruses," *Science*, vol. 272, no. 5258, pp. 74–79, 1996.

[5] A. S. Perelson and P. W. Nelson, "Mathematical analysis of HIV-1 dynamics in vivo," *SIAM Review*, vol. 41, no. 1, pp. 3–44, 1999.

[6] A. S. Perelson, "Modelling viral and immune system dynamics," *Nature Reviews Immunology*, vol. 2, no. 1, pp. 28–36, 2002.

[7] D. Wodarz and M. A. Nowak, "Mathematical models of HIV pathogenesis and treatment," *BioEssays*, vol. 24, no. 12, pp. 1178–1187, 2002.

[8] T. Kajiwara, T. Sasaki, and Department of Environmental and Mathematical Science, Okayama University, 700-8530 Tsushima, Okayama, "A note on the stability analysis of pathogen-immune interaction dynamics," *Discrete and Continuous Dynamical Systems, Series B*, vol. 4, no. 3, pp. 615–622, 2004.

[9] A. Murase, T. Sasaki, and T. Kajiwara, "Stability analysis of pathogen-immune interaction dynamics," *Journal of Mathematical Biology*, vol. 51, no. 3, pp. 247–267, 2005.

[10] Y. Tian and X. Liu, "Global dynamics of a virus dynamical model with general incidence rate and cure rate," *Nonlinear Analysis: Real World Appllication*, vol. 16, pp. 17–26, 2014.

[11] D. Wodarz, J. P. Christensen, and A. R. Thomsen, "The importance of lytic and nonlytic immune responses in viral infections," *Trends in Immunology*, vol. 23, no. 4, pp. 194–200, 2002.

[12] S. Bera, S. Khajanchi, and T. K. Roy, "Stability analysis of fuzzy HTLV-I infection model: a dynamic approach," *Journal of Applied Mathematics and Computing*, 2022.

[13] A. B. Balazs, J. Chen, C. M. Hong, D. S. Rao, L. Yang, and D. Baltimore, "Antibody-based protection against HIV infection by vectored immunoprophylaxis," *Nature*, vol. 481, no. 7379, pp. 81–84, 2012.

[14] X. Wang and W. Wang, "An HIV infection model based on a vectored immunoprophylaxis experiment," *Journal of Theoretical Biology*, vol. 313, pp. 127–135, 2012.

[15] F. Bagnoli, P. Liò, and L. Sguanci, "Modeling viral coevolution: HIV multi-clonal persistence and competition dynamics," *Physica A: Statistical Mechanics and its Applications*, vol. 366, pp. 333–346, 2006.

[16] O. Krakovska and L. M. Wahl, "Costs versus benefits: best possible and best practical treatment regimens for HIV," *Journal of Mathematical Biology*, vol. 54, no. 3, pp. 385–406, 2007.

[17] S. Bera, S. Khajanchi, and T. K. Roy, "Dynamics of an HTLV-I infection model with delayed CTLs immune response," *Applied Mathematics and Computation*, vol. 430, article 127206, 2022.

[18] K. Allali and S. Harroudi, "Modelling the adaptive immune response in HIV infection with three saturated rates and therapy," in *Trends in Biomathematics: Modeling*, R. Mondaini, Ed., Optimization and Computational Problems, Springer Cham, 2018.

[19] J. Danane and K. Allali, "Mathematical analysis and clinical implications of an HIV model with adaptive immunity," *Computational and Mathematical Methods in Medicine*, vol. 2019, Article ID 7673212, 19 pages, 2019.

[20] J. Luo, W. Wang, H. Chen, and R. Fu, "Bifurcations of a mathematical model for HIV dynamics," *Journal of Mathematical Analysis and Applications*, vol. 434, no. 1, pp. 837–857, 2016.

[21] J. Luo and Y. Zhao, "Dynamic behavioral analysis of an HIV model incorporating immune responses," *International Journal of Bifurcation and Chaos*, vol. 29, no. 9, article 1950120, 2019.

[22] Y. Yuan and L. J. Allen, "Stochastic models for virus and immune system dynamics," *Mathematical Biosciences*, vol. 234, no. 2, pp. 84–94, 2011.

[23] P. van den Driessche and J. Watmough, "Reproduction numbers and sub-threshold endemic equilibria for compartmental models of disease transmission," *Mathematical Biosciences*, vol. 180, no. 1-2, pp. 29–48, 2002.

[24] A. Dhooge, W. Govaerts, and Y. A. Kuznetsov, "MATCONT," *ACM Trans. Math. Software*, vol. 29, no. 2, pp. 141–164, 2003.

[25] A. Dhooge, W. Govaerts, Y. A. Kuznetsov, H. G. E. Meijer, and B. Sautois, "New features of the software MatContfor bifurcation analysis of dynamical systems," *Mathematical and Computer Modelling of Dynamical Systems*, vol. 14, no. 2, pp. 147–175, 2008.